

Overexpression of eNOS in brain stem reduces enhanced sympathetic drive in mice with myocardial infarction

Koji Sakai, Yoshitaka Hirooka, Hideaki Shigematsu, Takuya Kishi,
Koji Ito, Hiroaki Shimokawa, Akira Takeshita, and Kenji Sunagawa

Department of Cardiovascular Medicine, Kyushu University Graduate School of Medical Sciences, Fukuoka, Japan

Submitted 25 April 2005; accepted in final form 5 July 2005

Sakai, Koji, Yoshitaka Hirooka, Hideaki Shigematsu, Takuya Kishi, Koji Ito, Hiroaki Shimokawa, Akira Takeshita, and Kenji Sunagawa. Overexpression of eNOS in brain stem reduces enhanced sympathetic drive in mice with myocardial infarction. *Am J Physiol Heart Circ Physiol* 289: H2159–H2166, 2005. First published July 8, 2005; doi:10.1152/ajpheart.00408.2005.—Reduced nitric oxide (NO) in the brain might contribute to enhanced sympathetic drive in heart failure (HF). The aim of this study was to determine whether increased NO production induced by local overexpression of endothelial NO synthase (eNOS) in the nucleus tractus solitarius (NTS) of the brain stem reduces the enhanced sympathetic drive in mice with HF. Myocardial infarction (MI) was induced in mice by ligating the left coronary artery. MI mice exhibited left ventricular dilatation and a reduced left ventricular ejection fraction. Urinary norepinephrine excretion in MI mice was greater than that in sham-operated mice, indicating that sympathetic drive was enhanced in this model. Thus this model has features that are typical of HF. Western blot analysis and immunohistochemical staining for neuronal NOS (nNOS) indicated that nNOS protein expression was significantly reduced in the brain stem of MI mice. MI mice had a significantly smaller increase in blood pressure evoked by intracisternal injection of N^G -monomethyl-L-arginine than sham-operated mice. Adenoviral vectors encoding either eNOS (AdeNOS) or β -galactosidase (Ad β gal) were transfected into the NTS to examine the effect of increased NO production in the NTS on the enhanced sympathetic drive in HF. After the gene transfer, urinary norepinephrine excretion was reduced in AdeNOS-transfected MI mice but not in Ad β gal-transfected MI mice. These results indicate that nNOS expression in the brain stem, especially in the NTS, is reduced in the MI mouse model of HF, and increased NO production induced by overexpression of eNOS in the NTS attenuates the enhanced sympathetic drive in this model.

nitric oxide; heart failure; brain; sympathetic; genes

CHRONIC HEART FAILURE (HF) is characterized by enhanced neurohumoral drive in experimental animals as well as in patients (27, 29, 55). Sympathetic and humoral activation precede the onset of clinically recognized HF (11). In particular, there is accumulating evidence that β -blockers are one of the most effective drugs for treatment of patients with chronic HF (3, 31, 48), supporting the idea that the activation of the sympathetic nervous system has an important role in the progression of HF. In fact, plasma norepinephrine levels increase in relation to the severity of HF and correlate with mortality rates in patients with chronic HF (4, 38). The exact mechanisms underlying sympathoexcitation in HF are not clear, although several mechanisms have been proposed. Recent studies (27, 29, 55) suggest that the central nervous system

(CNS) is involved in the mechanism(s) underlying sympathoexcitation in HF.

The nucleus tractus solitarius (NTS) in the brain stem is involved in regulating blood pressure, heart rate, and sympathetic nerve activity (1, 5, 23). The NTS receives inputs from afferent fibers arising from arterial baroreceptors, chemoreceptors, cardiopulmonary receptors, and other visceral receptors and thus has an important role in autonomic control of the cardiovascular system (1, 5, 23). There is considerable evidence that nitric oxide (NO) in the CNS, including the NTS, inhibits sympathetic nerve activity (14, 16, 33, 46, 52). In addition, there are high concentrations of neuronal NO synthase (nNOS) in brain stem regions, particularly in the NTS, as demonstrated by immunohistochemistry, NADPH-diaphorase staining, and autoradiography studies (7, 13, 47). Recent studies (18, 33, 50, 54) demonstrated reduced nNOS expression in the paraventricular nucleus (PVN) of the hypothalamus in a rat model of HF. Although the mRNA level of nNOS in the brain stem is reduced (33), the pathophysiological role of NO in the brain stem, particularly in the NTS, in HF is not known. Thus a more precise physiological investigation related to the NTS is necessary.

Therefore, we hypothesized that NOS in the brain stem, particularly in the NTS, is altered in HF, and this alteration contributes to the sympathoexcitation in the mouse model with HF. The aim of the present study was to determine whether endogenous nNOS in the brain stem is reduced in a mouse model of HF. Myocardial infarction (MI) was produced by left coronary artery (LCA) occlusion in mice to determine whether this model exhibits sympathoexcitation similar to that in human HF and changes in nNOS expression. Second, we transfected adenoviral vectors encoding endothelial NOS (AdeNOS) into the NTS to increase local NO production in the NTS of mice, using a technique previously established in rats (17, 22, 39). Urinary norepinephrine excretion was measured as a marker of the sympathetic nerve activity. We examined the effect of increased NO production induced by the transfection of AdeNOS in the NTS on sympathetic nerve activity.

METHODS

Animals and surgery. This study was reviewed and approved by the Committee on Ethics of Animal Experiments, Faculty of Medicine, Kyushu University, and conducted according to the *Guidelines for Animal Experiments of the Faculty of Medicine*, Kyushu University (Fukuoka, Japan). Male CD-1 mice (10 to 12 wk old, weight 30–40 g, Charles River Japan, Yokohama, Japan) underwent coronary artery

Address for reprint requests and other correspondence: Y. Hirooka, Dept. of Cardiovascular Medicine, Kyushu Univ. Graduate School of Medical Sciences, 3-1-1 Maidashi, Higashi-ku, Fukuoka 812-8582, Japan (e-mail: hyoshi@cardiol.med.kyushu-u.ac.jp).

The costs of publication of this article were defrayed in part by the payment of page charges. The article must therefore be hereby marked “advertisement” in accordance with 18 U.S.C. Section 1734 solely to indicate this fact.

ligation to produce MI. The surgical procedures are described in detail elsewhere (28). Briefly, after pentobarbital sodium anesthesia (25–40 mg/kg ip) and intubation with a polyethylene tube (size 60), animals were ventilated by using a volume-cycled rodent respirator with 2 to 3 ml/cycle at a respiratory rate of 120 breaths/min. After thoracotomy, the LCA was ligated with a suture, 3 to 4 mm from the tip of the left auricle. The chest wall and skin were closed with a suture. The same surgical procedures were performed in sham mice, except that the coronary artery was not ligated.

LV morphology and morphometry. Four weeks after LCA ligation, the left ventricle (LV), including the septum, and the right ventricle were dissected to confirm MI in some groups of mice. After the major long-axis intracavitary diameter was measured, each LV was serially sectioned into three rings perpendicular to the major axis of the heart, after which the short-axis diameter was measured. At the midregion, the minimal and maximal chamber diameters were used with the long-axis diameter to compute the LV chamber volume. Infarct size in these hearts was determined by the method described previously (40). Briefly, serial 5- μ m sections were prepared, mounted, and stained with Masson trichrome. Infarct length was measured along the endo- and epicardial surfaces from each of the three LV sections, and values from all three sections were summed. Total LV circumference was calculated as the sum of the endo- and epicardial segment lengths from all three sections. Infarct size (in %) was calculated as the total infarct circumference divided by the total circumference times 100.

Measurement of blood pressure and heart rate during intracisternal administration of L-NMMA. In a separate group of animals, we examined the effects of intracisternal injection of *N*^G-monomethyl-L-arginine (L-NMMA), a NOS inhibitor, on blood pressure in the MI and sham-operated mice ($n = 6$ mice each) to confirm that the NOS activity was altered in MI mice. Four weeks after LCA ligation, the mice were anesthetized with pentobarbital sodium (50 mg/kg ip) and mechanically ventilated with room air supplemented with oxygen. A catheter was introduced into the left femoral vein for the administration of anesthetics. Another catheter was introduced into the aorta through the femoral artery to monitor and record systemic arterial pressure. The mice were placed in a stereotaxic frame, the dorsal surface of the medulla was then exposed, and the tip of a polyethylene tube (PE-10) was placed into the cisterna magna. Bolus injections of L-NMMA (100 nmol, 10 μ l) were made through this tube. The drugs were dissolved in artificial cerebrospinal fluid containing (in mM) 123 NaCl, 0.86 CaCl₂, 3.0 KCl, 0.89 MgCl₂, 25 NaHCO₃, 0.5 NaH₂PO₄, and 0.25 Na₂HPO₄; pH 7.4.

Construction and purification of recombinant adenovirus. We used adenoviral vectors encoding either the bacterial β -galactosidase (Ad β gal) gene or bovine endothelial NOS (eNOS) gene (6, 30). A replication-deficient adenovirus encoding the bovine eNOS gene expressed from a long-terminal repeat of the *Rous sarcoma* virus as a promoter was generated by using standard methods from the University of Iowa Gene Transfer Vector Core (Iowa City, IA) (6, 30). These vectors were suspended in PBS with 3% sucrose and stored at -80°C until use.

In vivo gene transfer into NTS. Four weeks after LCA ligation, mice were anesthetized with pentobarbital sodium (25–40 mg/kg ip), placed on a stereotaxic frame, and the dorsal surface of the medulla was exposed. A glass micropipette (5 μ m, outer diameter) was filled with PBS containing Ad β gal or AdeNOS. Bilateral injections were made into the NTS. One microinjection site in each NTS was defined according to a mouse atlas (35). An adenoviral suspension containing 1×10^8 plaque forming units per milliliter was injected into each injection site over 10 min (200 nl/each NTS; infusion rate, \sim 40 nl/min). After the injection, all mice recovered from the anesthesia and were unrestrained and free to move in their cages.

Histochemical analysis of β -galactosidase gene expression. On day 7 after the gene transfer, the mice were deeply anesthetized with pentobarbital sodium (100 mg/kg ip) and perfused transcardially with PBS, followed by 4% paraformaldehyde in PBS. The brains were

removed, and the coronal sections of the medulla were cut serially (50 μ m) using a vibratome. The sections of the medulla were evaluated for β -galactosidase expression by histostaining with X-Gal in PBS at 37°C for 4 h.

Quantification of β -galactosidase activity. We quantified β -galactosidase activity in the mice ($n = 4$ mice at each time point) transfected with Ad β gal with a colorimetric assay using *o*-nitrophenyl- β -D-galactopyranosidase (Boehringer Mannheim Biochemica; Mannheim, Germany) as described previously (2, 9, 17), before and on days 1, 3, 5, 7, 10, 14, 21, and 28 after the transfection of Ad β gal.

Immunohistochemistry for eNOS and nNOS. In another group of animals, sheep anti-nNOS antibody (kindly provided by P. Emson, Department of Neurobiology, The Babraham Institute, Cambridge, UK) was used for an immunohistochemical analysis of endogenous nNOS (19). Four weeks after LCA ligation, serial sections of the medulla were obtained. The sections were incubated in sheep anti-nNOS antibody (1:10,000) and then rinsed in PBS. After overnight incubation in biotinylated donkey anti-sheep IgG (1:1,000, Jackson; Baltimore, MD), the sections were rinsed in PBS and incubated in a mixture of streptavidin-conjugated fluorescein isothiocyanate (1:200; Vector; Burlingame, CA). After being rinsed in PBS, the sections were mounted in Vectashield (Vector). In a separate group of mice transfected with AdeNOS, we performed immunohistochemistry for eNOS as described previously (22, 39). On day 7 after the gene transfer, the sections were incubated in rabbit anti-eNOS IgG (1:200; Transduction; Lexington, KY) at room temperature overnight and then rinsed three times in PBS. After incubation with biotinylated horse anti-rabbit IgG (1:1,000, Vector), the sections were rinsed in PBS and incubated in a mixture of streptavidin-conjugated rhodamine (1:100, Vector). After being rinsed in PBS, the sections were mounted in Vectashield (Vector). The stained sections were photographed by using a confocal laser scanning microscope (MRC 1000, Bio-Rad; mounted on a Nikon light microscope Optiphot, Hemel Hempstead, UK) using laser beams of 488 nm for nNOS-stained sections and 580 nm for eNOS-stained sections for excitation with appropriate filter sets. Confocal images were then transferred to a personal computer and analyzed by using the National Institutes of Health Image program.

Western blot analysis for eNOS and nNOS. We performed Western blot analysis to determine the level of endogenous nNOS protein expression in MI mice. We also performed Western blot analysis to determine the time course of eNOS protein expression in AdeNOS-transfected mice. A coronal block of the brain ($n = 4$ mice for each line) containing the NTS was dissected, and the NTS tissues were obtained by using the punch microdissection technique (32, 33, 41) in MI mice and AdeNOS-transfected mice at 4 wk after LCA ligation and on days 0, 3, 5, 7, 10, 14, and 28 after AdeNOS transfer, respectively. The NTS tissues were homogenized and sonicated in a lysis buffer containing 40 mmol/l HEPES, 1% Triton X-100, 10% glycerol, and 1 mmol/l phenylmethylsulfonyl fluoride. The tissue lysate was centrifuged at 6,000 rpm for 5 min at 4°C using a microcentrifuge. The supernatant was collected, and the protein concentration was determined by using a bicinchoninic acid protein assay kit (Pierce Chemical; Rockford, IL). An aliquot of 5 μ g of protein from each sample was separated on a sodium dodecyl sulfate gel and transferred electrophoretically onto polyvinylidene difluoride membranes (Immobilon-P membrane; Millipore, Bedford, MA). After we confirmed that equal amounts of protein were applied into each well using Ponceau S (Sigma Chemical, St. Louis, MO) staining, the membranes were incubated with either sheep anti-nNOS antibody (1:10,000) in MI mouse samples or rabbit anti-eNOS (1:200) in AdeNOS-transfected mouse samples. Membranes were then washed and incubated with a horseradish peroxidase conjugated horse anti-sheep IgG antibody (1:10,000) or horse anti-rabbit IgG (1:100,000), respectively. Immunoreactivity was detected by enhanced chemiluminescence autoradiography (ECL Western blotting detection kit; Amersham; Arlington Heights, IL).

Echocardiographic imaging. Four weeks after LCA ligation, i.e., just before the adenoviral gene transfer, serial two-dimensional and M-mode echocardiography was performed in all groups of animals under light pentobarbital sodium anesthesia with spontaneous respiration (15). An echocardiography system (SSD5000; Aloka, Tokyo) was used with a dynamically focused 10-MHz linear array transducer using a depth setting of 200 mm, as described previously (15, 28). Two-dimensional images and M-mode tracings were recorded from the short-axis view at the level of the papillary muscle. Care was taken to avoid applying too much pressure to the chest wall. The M-mode tracings were printed on glossy paper using a digital color printer (SSZ337). LV end-diastolic diameter (LVEDD), LV end-systolic diameter (LVESD), and wall thickness were measured, and the mean of three-to-five cardiac cycles was used for analysis. Percent fractional shortening (%FS) was calculated as follows: $\%FS = (LVEDD) - (LVESD)/(LVEDD) \times 100$. The same echocardiographic experiments were performed 6 and 8 wk after LCA ligation, i.e., 2 and 4 wk after AdeNOS gene transfer, respectively.

Measurement of urinary norepinephrine excretion. The urinary norepinephrine concentration was measured 4 wk after LCA ligation, i.e., just before gene transfer, and 7 days after the gene transfer by high-performance liquid chromatography, and urinary norepinephrine excretion over 24 h ($\mu\text{g}/\text{day}$) was then calculated as described previously (17, 22, 39).

Statistical analysis. All values were expressed as means \pm SE. One-way ANOVA was used to compare the β -galactosidase activity. An unpaired *t*-test was used to compare values between the MI mice and sham-operated mice. Two-way ANOVA with repeated measures was used to compare the time course values of LVEDD and %FS between Ad β gal and AdeNOS-transfected MI mice groups. A paired *t*-test was used to compare the values before and after each operation, or before and after the gene transfer, in sham-operated and MI mice. Differences were considered to be significant when $P < 0.05$.

RESULTS

HF characteristics of MI mice. Echocardiographic assessment of cardiac function was performed, and infarct size was estimated using Masson trichrome staining before and 4 wk after LCA ligation. Echocardiographic evaluation revealed that LVEDD was greater (5.2 ± 0.4 vs. 3.6 ± 0.2 mm; $P < 0.01$) and fractional shortening was smaller ($19.1 \pm 0.2\%$ vs. $42.7 \pm 0.1\%$; $P < 0.01$) in MI mice than in sham-operated mice ($n = 11$, each group) (Fig. 1, *A* and *B*). Examples of coronal sections of the LV are shown in Fig. 1, *C* and *D*. Infarct size of MI mice was $42.5 \pm 2.3\%$ (see Fig. 1, *C* and *D*). Furthermore, 24-h urinary norepinephrine excretion was significantly higher in MI mice compared with that in sham-operated mice (MI mice, 0.33 ± 0.06 μg ; sham mice, 0.18 ± 0.03 μg ; $n = 13$ mice for each group, $P < 0.05$). There was no difference in 24-h urinary volume between MI mice and sham-operated mice (data not shown).

Brain stem nNOS is reduced in HF. In this model, we evaluated nNOS protein expression in the brain stem by Western blot analysis and immunohistochemistry 4 wk after LCA ligation. Western blot analysis for nNOS in the NTS revealed reduced nNOS protein levels in MI mice compared with sham-operated mice (Fig. 2*A*). Immunohistochemical staining for nNOS protein was reduced in MI mice compared with that in sham-operated mice (Fig. 2, *B* and *C*).

Effect of intracisternal injection of L-NMMA on blood pressure. To determine whether endogenous NOS activity was altered in MI mice, we examined the effects of intracisternal injection of L-NMMA on blood pressure in sham-operated and

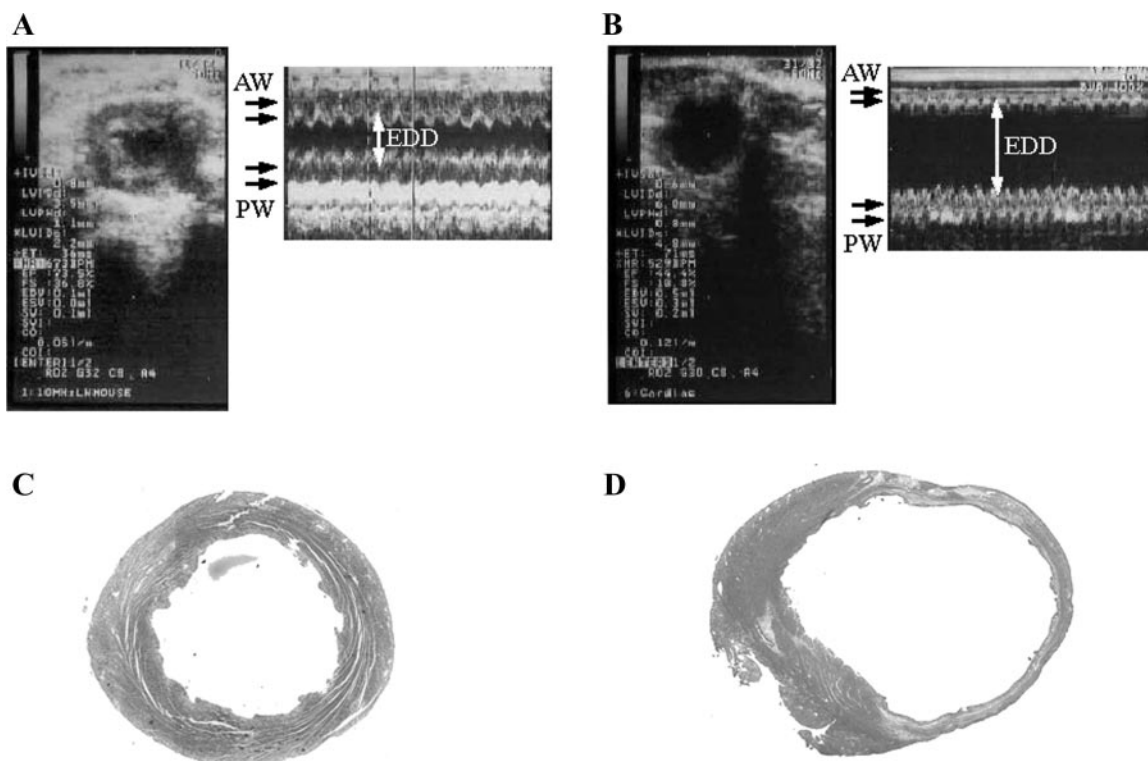


Fig. 1. B-mode and M-mode echocardiograms of left ventricular (LV) in parasternal short-axis view obtained from sham-operated (*A*) and myocardial infarction (MI) (*B*) mice. EDD, end-diastolic diameter; AW, anterior wall; PW posterior wall. MI mice exhibited LV dilatation and decreased fractional shortening. Low-power photograph of Masson-trichrome-stained LV cross-section was obtained from sham-operated (*C*) and MI (*D*) mice.

MI mice. Intracisternal injection of L-NMMA elicited a smaller increase in blood pressure in MI mice than in sham-operated mice (6.9 ± 3.4 vs. 20.6 ± 4.9 mmHg; $P < 0.05$) (Fig. 3B).

Effect of eNOS overexpression in NTS. Figure 4A shows the X-Gal staining for β -galactosidase in a section of the mouse brain medulla on *day 7* after the gene transfer. Positive staining for β -galactosidase was observed in the NTS where Ad β gal had been microinjected. In the AdeNOS-transfected mice, eNOS protein expression was observed immunohistochemically in the NTS where AdeNOS had been microinjected (Fig. 4B). Figure 4C shows the time course of β -galactosidase

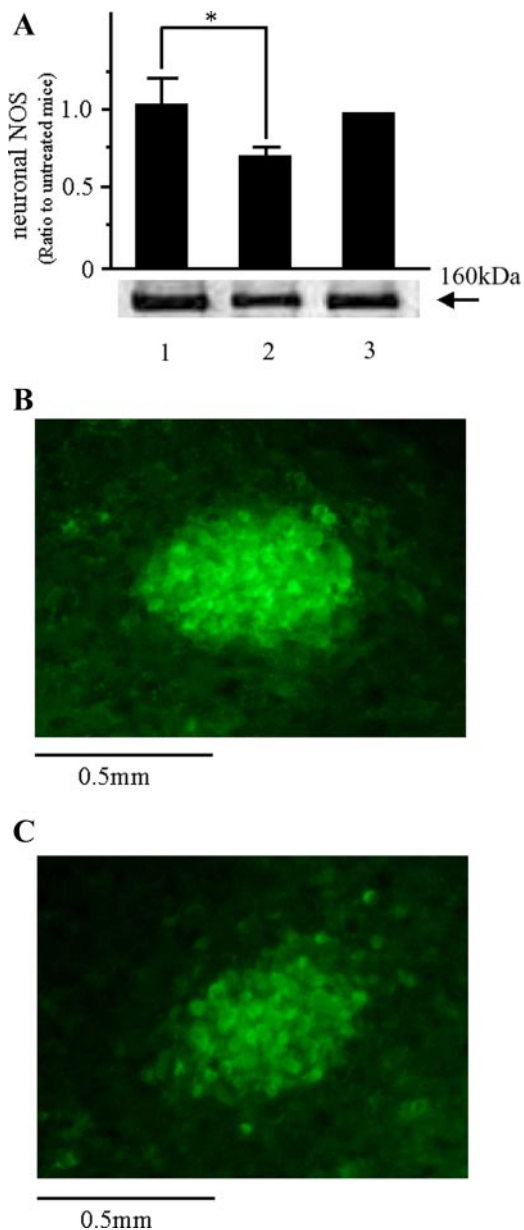


Fig. 2. Western blot analysis in nucleus tractus solitarius (NTS) demonstrating reduction in endogenous neuronal nitric oxide synthase (nNOS) protein in MI mice ($n = 4$ mice for each) *A*: lane 1, sham-operated mouse; lane 2, MI mouse; lane 3, untreated mouse. Immunohistochemical staining visualized with rhodamine-conjugated fluorophore for endogenous nNOS protein within NTS tissue in sham-operated (*B*) and MI (*C*) mice. $*P < 0.05$ compared with the value of sham-operated mice.

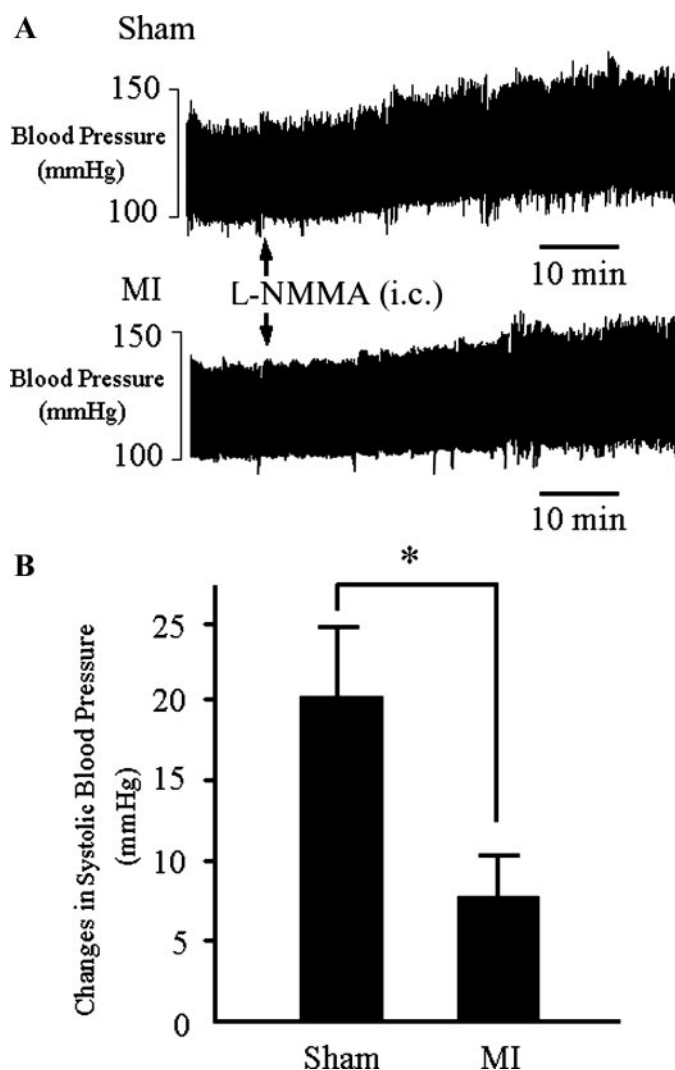


Fig. 3. Typical effects (*A*) and summary (*B*) observed in blood pressure changes after intracisternal (i.c.) injection of N^G -monomethyl-L-arginine (L-NMMA) in sham-operated and MI (*B*) mice, suggesting that NOS activity was reduced in MI mice ($n = 6$ mice for each, $*P < 0.05$).

activity before and after Ad β gal transfection. The β -galactosidase activity in the medulla peaked on *day 7* and then declined over time. Figure 4D shows the time course of eNOS protein expression as determined by Western blot analysis. eNOS protein expression peaked at *day 7* and then declined over time until *day 28*. Urinary norepinephrine excretion in MI mice transfected with Ad β gal or AdeNOS was also measured. Urinary norepinephrine excretion did not differ before adenoviral gene transfer (Fig. 5). Urinary norepinephrine excretion after transfection with AdeNOS, however, was significantly lower than before transfection with AdeNOS. In addition, after the gene transfer, urinary norepinephrine excretion in AdeNOS-transfected MI mice was significantly lower than in Ad β gal-transfected MI mice. There was no change in 24-h urinary volume after AdeNOS transfection (data not shown). Adenoviral-mediated eNOS gene delivery did not improve the LV systolic function determined by EDD and %FS (Table 1).

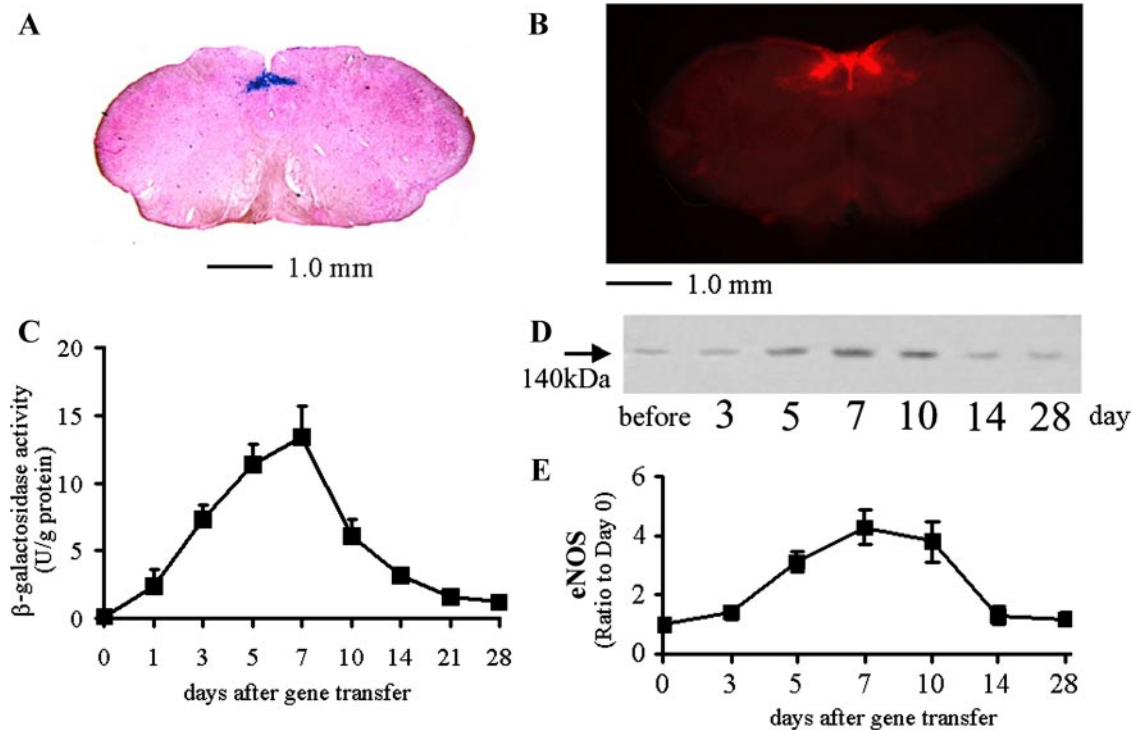


Fig. 4. Site-specific expression of β -galactosidase or endothelial NOS (eNOS) protein within NTS. *A*: dark blue X-Gal staining was observed locally in NTS of Ad β gal-transfected mice. *B*: images of section of medulla stained with anti-eNOS antibody (red, visualized with rhodamine-conjugated fluorophore). *C*: eNOS-immunopositive sites are also detected locally in bilateral NTS of AdeNOS-injected mice. Time course of β -galactosidase activity in medulla transfected with Ad β gal. β -Galactosidase activity was quantified by using colorimetric assay ($n = 4$ mice at each time point). *D* and *E*: time course of eNOS protein expression in medulla transfected with AdeNOS by Western blot analysis.

DISCUSSION

The major findings of the present study are as follows. First, the characteristics of MI mice were consistent with those of HF, a particularly increased activation of the sympathetic nervous system as determined by an increase in urinary norepinephrine excretion. Second, nNOS expression levels were significantly reduced in this MI mouse model. Finally, increased NO production induced by eNOS overexpression in the NTS in MI mice reduced urinary norepinephrine excretion to the levels of the sham-operated mice, suggesting that increased NO production in the NTS reduced the enhanced sympathetic

drive in MI mice. Taken together, these results indicate that decreased NO in the brain, especially in the NTS, contributes to the enhanced sympathetic drive observed in HF.

MI mouse model of HF. HF was produced by coronary artery ligation in mice. This model is often used as a model of LV remodeling, myocardial ischemia, and reperfusion injury (15, 24, 28, 36, 39, 40, 43). Little is known, however, regarding the neurohumoral aspects of this model in mice. In our study, we demonstrated that urinary norepinephrine excretion measured

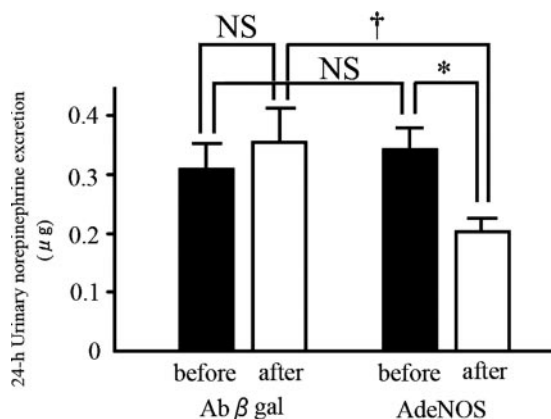


Fig. 5. Twenty-four-hour urinary norepinephrine excretion (in μ g) before and after gene transfer in AdeNOS- and Ad β gal-transfected MI mice. NS, not significant. * $P < 0.05$; † $P < 0.01$.

Table 1. Time course of LV end-diastolic diameter and %FS in MI and sham-operated mice transfected with either Ad β gal or AdeNOS

	Sham Mice		MI Mice	
	AdeNOS	Ad β gal	AdeNOS	Ad β gal
<i>n</i>	10	7	9	6
<i>LV end-diastolic diameter, mm</i>				
Before LCA Ligation	3.7 \pm 0.2	3.6 \pm 0.2	5.3 \pm 0.3	5.2 \pm 0.4
2 Wk	3.6 \pm 0.3	3.7 \pm 0.3	5.3 \pm 0.4	5.4 \pm 0.6
4 Wk	3.8 \pm 0.3	3.8 \pm 0.3	4.9 \pm 0.5	5.2 \pm 0.9
<i>%FS</i>				
Before LCA Ligation	45.5 \pm 0.2	42.7 \pm 0.3	19.7 \pm 0.9	19.1 \pm 0.9
4 Wk	44.2 \pm 0.3	44.9 \pm 0.3	22.7 \pm 1.2	20.8 \pm 1.7
8 Wk	39.1 \pm 0.4	40.5 \pm 0.3	24.7 \pm 1.4	19.3 \pm 1.5

Values are means \pm SE; *n*, number of mice. LV, left ventricular; % FS, percent fractional shortening; MI, myocardial infarction; Ad β gal and AdeNOS, adenoviral vectors encoding β -galactosidase or endothelial nitric oxide synthase, respectively.

in a conscious state, which is a marker of sympathetic nerve activity, was significantly increased in mice 4 wk after MI. Consistent with the results of previous studies from Takeshita's laboratory (15), LV dilatation and reduced LV systolic function were also observed.

Sympathoexcitation in HF and role of NO in brain stems. HF is characterized by an enhanced neurohumoral drive in experimental animals as well as in patients (27, 29, 55). In patients with HF, plasma norepinephrine levels increase with severity and relate to the mortality rate (4, 38). The mechanism(s) underlying the sympathoexcitation observed in HF is not fully understood. Although it has been thought that abnormal arterial baroreflex and cardiopulmonary baroreflex control of sympathetic nerve activity are responsible for the sympathoexcitation in HF, recent studies (27, 29, 55) suggest that involvement of the CNS is important. Many studies (10, 27, 29, 55) predict an important role of angiotensin II, particularly in the forebrain, in HF. Liu and Zucker (25) suggested that a loss of NO and an increase in angiotensin II are necessary for sustained increases in sympathetic nerve activity in HF. In fact, inhibition of angiotensin II type I receptors in the NTS reduces arterial blood pressure, heart rate, and sympathetic nerve activity in rats with chronic inhibition of NOS (8). Previous studies from our laboratories and others (17, 22, 39) have established that NO in the brain inhibits sympathetic nerve activity. There are few studies (34, 54), however, regarding NO in the brain, especially the NTS, in HF. Patel et al. (33) reported decreased nNOS gene mRNA expression levels in the hypothalamus, dorsal pons, and dorsal medulla of rats with MI compared with those in sham-operated rats. In addition, the number of NADPH-diaphorase-positive neurons, a marker of nNOS activity, was significantly decreased in the PVN (54). In animal models of HF, blunted NO inhibition mediated sympathoexcitation in the PVN (53) and reduced central NO-mediated enhanced sympathetic afferent baroreflex gain (26).

In the present study, nNOS expression evaluated by Western blot analysis and immunohistochemical staining in the brain stem, particularly in the NTS, was reduced in HF mice compared with that in sham-operated mice. Also, the pressor response evoked by intracisternal injection of L-NMMA was lower in MI mice compared with that in sham-operated mice, suggesting that NOS activity in the NTS is reduced in our MI mouse model.

Effect of eNOS overexpression in NTS. The most important finding of the present study is that the increase in urinary norepinephrine excretion in MI mice was significantly reduced compared with that in the sham-operated mice after eNOS overexpression in the NTS in a conscious state. This finding indicates that an increase in NO production in the NTS normalizes the enhanced sympathetic drive observed in HF. In the present study, we transfected adenoviral vectors encoding either the β -galactosidase gene or the eNOS gene into the NTS of mice in vivo, which was confirmed by Western blot analysis and immunohistochemical staining. Furthermore, consistent with previous studies from Takeshita's laboratory (39) using rats, the time course of β -galactosidase activity or eNOS expression peaked on *day 7* after the gene transfer. Because we (20) and others (44) previously demonstrated that overexpression of eNOS in the brain does not affect the nNOS expression levels, the maximum physiological effect of viral-mediated gene transfer was anticipated to occur on *day 7* after the gene

transfer. Therefore, we measured urinary norepinephrine excretion on *day 7* after the gene transfer. As discussed in previous studies (17, 22, 39) using this technique, we used eNOS instead of nNOS, which normally exists in the CNS, because the purpose of this study was to increase the local NO production in the NTS for a relatively long period in mice transfected with AdeNOS. We previously demonstrated that this method is useful for examining the effect of NO overproduction in a specific nucleus of the brain on cardiovascular regulation in conscious animals (17, 22, 39). The increase in NOS expression in the NTS attenuated the increase in urinary norepinephrine excretion, which is a marker of sympathetic nerve activity, in MI mice in a conscious state. These results suggest that the reduced NO production in the NTS contributes to the enhanced sympathetic drive in HF.

Waki et al. (49) reported that chronic inhibition of endogenous eNOS in the caudal NTS enhances baroreflex and suggested that NO might be functionally diverse within the NTS. In the present study, we did not address the role of endogenous NO released from neurons and endothelium (34) on the baroreflex function in HF. There are functionally discrete subregions that exhibit a different response to the same neuropeptide, even within the NTS (45). Thus various results between the caudal subregion of the NTS in the study by Waki et al. (49) and the entire NTS in the present study might reflect the diverse physiological functions of NO based on discrete subgroups of neurons within the NTS.

A recent study (51) indicated that NO in a different brain stem nucleus, the rostral ventrolateral medulla, also improves HF pathophysiology. Therefore, increasing NO in the brain stem might be a new therapeutic target for the treatment of HF from the aspect of neurohumoral activation.

Study limitations. It is possible that the reduced blood pressure response to L-NMMA in mice with HF was due to elevated basal sympathetic nerve activity that cannot be further increased. This possibility is unlikely, however, because the sympathetic nerve response to blocking the airway in HF rats was higher than that elicited by L-NMMA (53). Recently, it was suggested that NADPH-dependent superoxide anions are increased in the brain in experimental chronic HF and that increased reactive oxygen species in the brain contribute to increased sympathetic nerve activity (12, 21, 24). Because brain NO might be trapped by increased superoxide anions in chronic HF states, it is possible that the sympathoexcitation in HF is determined by the balance between NO and reactive oxygen species. Further studies are required to elucidate this point.

We found that eNOS gene transfer in the NTS normalized the enhanced sympathetic drive observed in our HF model. We measured urinary norepinephrine excretion as a marker of sympathetic nerve activity. Direct measurement of sympathetic nerve activity is preferable, but it is technically difficult to perform in conscious mice. Because the expression of the gene using adenovirus vectors remains high enough for only several days, this technique does not allow us to observe an improvement in survival (data not shown) or inhibition of LV remodeling (Table 1). Further experiments to examine the long-term effect of an increase in NO within the brain stem in HF are important. Another efficient vector system that expresses the gene for a longer period, such as the adenovirus-associated virus (37) or feline immunodeficiency virus (42),

might be useful for examining the long-term effect of NO in the NTS on HF.

In conclusion, MI mice have characteristics consistent with HF, particularly from the aspect of sympathetic nervous system activation. This activation is mediated, at least in part, by decreases in nNOS expression, resulting in decreased NO production in the NTS. Overexpression of eNOS in the NTS decreases urinary norepinephrine excretion, suggesting that increased NO production in the brain stem, particularly in the NTS, reduces the enhanced sympathetic drive observed in HF.

ACKNOWLEDGMENTS

The authors thank Drs. D. D. Heistad and B. L. Davidson (The University of Iowa Gene Transfer Vector Core, supported by National Institutes of Health grants and the Carver Foundation) for the preparation of vectors. We thank Dr. P. Emson for kindly providing the sheep antibody to nNOS. We also thank Dr. T. Kosaka for advice in the immunohistochemical analysis for eNOS and the use of his facility for microscopic analysis.

GRANTS

This work was supported by a Grant-in-Aid for Scientific Research (C11670689) from the Ministry of Education, Science, Sports, and Culture and the Japan Society for the Promotion of Science.

REFERENCES

- Andresen MC and Kunze DL. Nucleus tractus solitarius—gateway to neural circulatory control. *Annu Rev Physiol* 56: 93–116, 1994.
- Bradford MM. A rapid and sensitive method for the quantitation of microgram quantities of protein utilizing the principle of protein-dye binding. *Anal Biochem* 72: 248–254, 1976.
- Bristow MR, O'Connell JB, Gilbert EM, French WJ, Leatherman G, Kantrowitz NE, Orié J, Smucker ML, Marshall G, and Kelly P. Dose-response of chronic beta-blocker treatment in heart failure from either idiopathic dilated or ischemic cardiomyopathy. Bucindolol Investigators. *Circulation* 89: 1632–1642, 1994.
- Cohn JN, Levine TB, Olivari MT, Garberg V, Lura D, Francis GS, Simon AB, and Rector T. Plasma norepinephrine as a guide to prognosis in patients with chronic congestive heart failure. *N Engl J Med* 311: 819–823, 1984.
- Dampney RA. Functional organization of central pathways regulating the cardiovascular system. *Physiol Rev* 74: 323–364, 1994.
- Davidson BL, Allen ED, Kozarsky KF, Wilson JM, and Roessler BJ. A model system for in vivo gene transfer into the central nervous system using an adenoviral vector. *Nat Genet* 3: 219–223, 1993.
- De Vente J, Hopkins DA, Markerink-Van Ittersum M, Emson PC, Schmidt HH, and Steinbusch HW. Distribution of nitric oxide synthase and nitric oxide-receptive, cyclic GMP-producing structures in the rat brain. *Neuroscience* 87: 207–241, 1998.
- Eshima K, Hirooka Y, Shigematsu H, Matsuo I, Koike G, Sakai K, and Takeshita A. Angiotensin in the nucleus tractus solitarii contributes to neurogenic hypertension caused by chronic nitric oxide synthase inhibition. *Hypertension* 36: 259–263, 2000.
- Eustice DC, Feldman PA, Colberg-Poley AM, Buckery RM, and Neubauer RH. A sensitive method for the detection of beta-galactosidase in transfected mammalian cells. *Biotechniques* 11: 739–740, 1991.
- Felder RB, Francis J, Weiss RM, Zhang ZH, Wei SG, and Johnson AK. Neurohumoral regulation in ischemia-induced heart failure. Role of the forebrain. *Ann NY Acad Sci* 940: 444–453, 2001.
- Francis GS, Benedict C, Johnstone DE, Kirlin PC, Nicklas J, Liang CS, Kubo SH, Rudin-Toretzky E, and Yusuf S. Comparison of neuroendocrine activation in patients with left ventricular dysfunction with and without congestive heart failure. A substudy of the Studies of Left Ventricular Dysfunction (SOLVD). *Circulation* 82: 1724–1729, 1990.
- Gao L, Wang W, Li YL, Schultz HD, Liu D, Cornish KG, and Zucker IH. Superoxide mediates sympathoexcitation in heart failure: roles of angiotensin II and NAD(P)H oxidase. *Circ Res* 95: 937–944, 2004.
- Hara H, Waeber C, Huang PL, Fujii M, Fishman MC, and Moskowitz MA. Brain distribution of nitric oxide synthase in neuronal or endothelial nitric oxide synthase mutant mice using [³H]L-N^G-nitro-arginine autoradiography. *Neuroscience* 75: 881–890, 1996.
- Harada S, Tokunaga S, Momohara M, Masaki H, Tagawa T, Imaizumi T, and Takeshita A. Inhibition of nitric oxide formation in the nucleus tractus solitarius increases renal sympathetic nerve activity in rabbits. *Circ Res* 72: 511–516, 1993.
- Hayashidani S, Tsutsui H, Shiomi T, Suematsu N, Kinugawa S, Ide T, Wen J, and Takeshita A. Fluvastatin, a 3-hydroxy-3-methylglutaryl coenzyme A reductase inhibitor, attenuates left ventricular remodeling and failure after experimental myocardial infarction. *Circulation* 105: 868–873, 2002.
- Hironaga K, Hirooka Y, Matsuo I, Shihara M, Tagawa T, Harasawa Y, and Takeshita A. Role of endogenous nitric oxide in the brain stem on the rapid adaptation of baroreflex. *Hypertension* 31: 27–31, 1998.
- Hirooka Y, Sakai K, Kishi T, and Takeshita A. Adenovirus-mediated gene transfer into the NTS in conscious rats. A new approach to examining the central control of cardiovascular regulation. *Ann NY Acad Sci* 940: 197–205, 2001.
- Hirooka Y, Shigematsu H, Kishi T, Kimura Y, Ueta Y, and Takeshita A. Reduced nitric oxide synthase in the brain stem contributes to enhanced sympathetic drive in rats with heart failure. *J Cardiovasc Pharmacol* 42, Suppl 1: S111–S115, 2003.
- Jinno S, Aika Y, Fukuda T, and Kosaka T. Quantitative analysis of neuronal nitric oxide synthase-immunoreactive neurons in the mouse hippocampus with optical disector. *J Comp Neurol* 410: 398–412, 1999.
- Kishi T, Hirooka Y, Ito K, Sakai K, Shimokawa H, and Takeshita A. Cardiovascular effects of overexpression of endothelial nitric oxide synthase in the rostral ventrolateral medulla in stroke-prone spontaneously hypertensive rats. *Hypertension* 39: 264–268, 2002.
- Kishi T, Hirooka Y, Kimura Y, Ito K, Shimokawa H, and Takeshita A. Increased reactive oxygen species in rostral ventrolateral medulla contribute to neural mechanisms of hypertension in stroke-prone spontaneously hypertensive rats. *Circulation* 109: 2357–2362, 2004.
- Kishi T, Hirooka Y, Sakai K, Shigematsu H, Shimokawa H, and Takeshita A. Overexpression of eNOS in the RVLM causes hypotension and bradycardia via GABA release. *Hypertension* 38: 896–901, 2001.
- Kumada M, Terui N, and Kuwaki T. Arterial baroreceptor reflex: its central and peripheral neural mechanisms. *Prog Neurobiol* 35: 331–361, 1990.
- Lindley TE, Doobay MF, Sharma RV, and Davison RL. Superoxide is involved in the central nervous system activation and sympathoexcitation of myocardial infarction-induced heart failure. *Circ Res* 94: 402–409, 2004.
- Liu JL and Zucker IH. Regulation of sympathetic nerve activity in heart failure: a role for nitric oxide and angiotensin II. *Circ Res* 84: 417–423, 1999.
- Ma R, Zucker IH, and Wang W. Reduced NO enhances the central gain of cardiac sympathetic afferent reflex in dogs with heart failure. *Am J Physiol Heart Circ Physiol* 276: H19–H26, 1999.
- Mark AL. Sympathetic dysregulation in heart failure: mechanisms and therapy. *Clin Cardiol* 18: 13–18, 1995.
- Michael LH, Entman ML, Hartley CJ, Youker KA, Zhu J, Hall SR, Hawkins HK, Berens K, and Ballantyne CM. Myocardial ischemia and reperfusion: a murine model. *Am J Physiol Heart Circ Physiol* 269: H2147–H2154, 1995.
- Middlekauff HR and Mark AL. The treatment of heart failure: the role of neurohumoral activation. *Intern Med* 37: 112–122, 1998.
- Ooboshi H, Chu Y, Rios CD, Faraci FM, Davidson BL, and Heistad DD. Altered vascular function after adenovirus-mediated overexpression of endothelial nitric oxide synthase. *Am J Physiol Heart Circ Physiol* 273: H265–H270, 1997.
- Packer M, Bristow MR, Cohn JN, Colucci WS, Fowler MB, Gilbert EM, and Shusterman NH. The effect of carvedilol on morbidity and mortality in patients with chronic heart failure. U.S. Carvedilol Heart Failure Study Group. *N Engl J Med* 334: 1349–1355, 1996.
- Palkovits M. Punch sampling biopsy technique. *Methods Enzymol* 103: 368–376, 1983.
- Patel KP, Zhang K, Zucker IH, and Krukoff TL. Decreased gene expression of neuronal nitric oxide synthase in hypothalamus and brain stem of rats in heart failure. *Brain Res* 734: 109–115, 1996.
- Paton JF, Deuchars J, Ahmad Z, Wong LF, Murphy D, and Kasparov S. Adenoviral vector demonstrates that angiotensin II-induced depression of the cardiac baroreflex is mediated by endothelial nitric oxide synthase in the nucleus tractus solitarii of the rat. *J Physiol* 531: 445–458, 2001.

35. **Patrick RH, Warren GY, Floyd EB, Pavel VB, and Marco RC.** *Comparative Cytoarchitectonic Atlas of the C57BL/6 and 129/Sv Mouse Brains.* Amsterdam: Elsevier Science, 2000.
36. **Patten RD, Aronovitz MJ, Deras-Mejia L, Pandian NG, Hanak GG, Smith JJ, Mendelsohn ME, and Konstam MA.** Ventricular remodeling in a mouse model of myocardial infarction. *Am J Physiol Heart Circ Physiol* 274: H1812–H1820, 1998.
37. **Phillips MI.** Antisense inhibition and adeno-associated viral vector delivery for reducing hypertension. *Hypertension* 29: 177–187, 1997.
38. **Rector TS, Olivari MT, Levine TB, Francis GS, and Cohn JN.** Predicting survival for an individual with congestive heart failure using the plasma norepinephrine concentration. *Am Heart J* 114: 148–152, 1987.
39. **Sakai K, Hirooka Y, Matsuo I, Eshima K, Shigematsu H, Shimokawa H, and Takeshita A.** Overexpression of eNOS in NTS causes hypotension and bradycardia in vivo. *Hypertension* 36: 1023–1028, 2000.
40. **Scherrer-Crosbie M, Steudel W, Ullrich R, Hunziker PR, Liel-Cohen N, Newell J, Zaroff J, Zapol WM, and Picard MH.** Echocardiographic determination of risk area size in a murine model of myocardial ischemia. *Am J Physiol Heart Circ Physiol* 277: H986–H992, 1999.
41. **Shigematsu H, Hirooka Y, Eshima K, Shihara M, Tagawa T, and Takeshita A.** Endogenous angiotensin II in the NTS contributes to sympathetic activation in rats with aortocaval shunt. *Am J Physiol Regul Integr Comp Physiol* 280: R1665–R1673, 2001.
42. **Sinnayah P, Lindley TE, Staber PD, Cassell MD, Davidson BL, and Davisson RL.** Selective gene transfer to key cardiovascular regions of the brain: comparison of two viral vector systems. *Hypertension* 39: 603–608, 2002.
43. **Suzuki M, Sasaki N, Miki T, Sakamoto N, Ohmoto-Sekine Y, Tamagawa M, Seino S, Marban E, and Nakaya H.** Role of sarcolemmal K(ATP) channels in cardioprotection against ischemia/reperfusion injury in mice. *J Clin Invest* 109: 509–516, 2002.
44. **Tai MH, Wang LL, Wu KL, and Chan JY.** Increased superoxide anion in rostral ventrolateral medulla contributes to hypertension in spontaneously hypertensive rats via interactions with nitric oxide. *Free Radic Biol Med* 38: 450–462, 2005.
45. **Tan PS, Potas JR, Killinger S, Horiuchi J, Goodchild AK, Pilowsky PM, and Dampney RA.** Angiotensin II evokes hypotension and renal sympathoinhibition from a highly restricted region in the nucleus tractus solitarius. *Brain Res* 1036: 70–76, 2005.
46. **Tseng CJ, Liu HY, Lin HC, Ger LP, Tung CS, and Yen MH.** Cardiovascular effects of nitric oxide in the brain stem nuclei of rats. *Hypertension* 27: 36–42, 1996.
47. **Vincent SR and Kimura H.** Histochemical mapping of nitric oxide synthase in the rat brain. *Neuroscience* 46: 755–784, 1992.
48. **Waagstein F, Bristow MR, Swedberg K, Camerini F, Fowler MB, Silver MA, Gilbert EM, Johnson MR, Goss FG, and Hjalmarson A.** Beneficial effects of metoprolol in idiopathic dilated cardiomyopathy. Metoprolol in Dilated Cardiomyopathy (MDC) Trial Study Group. *Lancet* 342: 1441–1446, 1993.
49. **Waki H, Kasparov S, Wong LF, Murphy D, Shimizu T, and Paton JF.** Chronic inhibition of endothelial nitric oxide synthase activity in nucleus tractus solitarius enhances baroreceptor reflex in conscious rats. *J Physiol* 546: 233–242, 2003.
50. **Wang Y, Liu XF, Cornish KG, Zucker IH, and Patel KP.** Effects of nNOS antisense in the paraventricular nucleus on blood pressure and heart rate in rats with heart failure. *Am J Physiol Heart Circ Physiol* 288: H205–H213, 2005.
51. **Wang Y, Patel KP, Cornish KG, Channon KM, and Zucker IH.** nNOS gene transfer to RVLM improves baroreflex function in rats with chronic heart failure. *Am J Physiol Heart Circ Physiol* 285: H1660–H1667, 2003.
52. **Zanzinger J, Czachurski J, and Seller H.** Inhibition of sympathetic vasoconstriction is a major principle of vasodilation by nitric oxide in vivo. *Circ Res* 75: 1073–1077, 1994.
53. **Zhang K, Li YF, and Patel KP.** Blunted nitric oxide-mediated inhibition of renal nerve discharge within PVN of rats with heart failure. *Am J Physiol Heart Circ Physiol* 281: H995–H1004, 2001.
54. **Zhang K, Zucker IH, and Patel KP.** Altered number of diaphorase (NOS) positive neurons in the hypothalamus of rats with heart failure. *Brain Res* 786: 219–225, 1998.
55. **Zucker IH, Wang W, Brandle M, Schultz HD, and Patel KP.** Neural regulation of sympathetic nerve activity in heart failure. *Prog Cardiovasc Dis* 37: 397–414, 1995.